A High-resolution Parameter Extraction Algorithm for Multiple Clusters Channels

Zihang Cheng*, Jorge Gomez-Ponce*†, Naveed A. Abbasi*, and Andreas F. Molisch*

*University of Southern California, Los Angeles, CA, USA
†ESPOL Polytechnic University, Guayaquil, Ecuador
Email: {zihangch, gomezpon, nabbasi, molisch}@usc.edu

***Abstract*—Multi-path components (MPCs) in wireless channels generally occur in clusters, i.e., groups of MPCs that have similar delay/angle characteristics. However, when those clusters are widely separated and have significantly different power, high-resolution parameter extraction (HRPE) algorithms based on serial interference cancellation, such as CLEAN, can miss some of the weaker clusters because they concentrate the path search in the strongest cluster. This effect can occur particularly in the presence of calibration error and/or diffuse scattering. To solve this problem, we propose a heuristic modification, Regional CLEAN (R-CLEAN), that employs cluster identification in the Fourier domain and limits the number of MPCs per cluster. We first demonstrate the effect, and the effectiveness of our proposed algorithm, on synthetic channels with calibration error or diffuse scattering. We then demonstrate it with a THz Multiple-Input-Multiple-Output (MIMO) measurement at 145 - 146 GHz. The proposed optimization and algorithm can thus be an essential step towards evaluating channels with multiple clusters.**

***Index Terms*—Channel estimation, high-resolution algorithms, optimization, THz analysis**

I. Introduction

While 5G is currently in the first phase of worldwide deployment, even more advanced (6G) systems are being considered and developed [1]. The fundamental performance limits and the actual performance of architecture designs and protocols are determined by the characteristics of the channels the systems operate in. Since new systems will (partly) operate on different frequencies and in new scenarios, new channel models are required. To be realistic and reliable, these models have to be based on or verified by channel measurements, also known as *channel sounding* [2, Chapter 8].

Although there are a variety of channel sounding techniques, a common feature is that - assuming Fourier-based evaluation - the resolution in delay and angle is limited due to the finite aperture in frequency (bandwidth) and space (antenna size). High-resolution parameter extraction (HRPE) algorithms can be used to achieve higher-than-Fourier resolution. The current methods of choice for evaluating most measurement campaigns are maximum-likelihood (ML) estimators for the parameters of the MPCs. Since full ML estimation is computationally intensive, various iterative implementations have been proposed as more practical solutions, such as SAGE [3] and RIMAX [4], [5], and CLEAN [6]–[8]. The latter is not only of importance as a stand-alone algorithm but also because it is often employed to initialize SAGE and RIMAX; note that as for most iterative algorithms, and especially for non-convex optimization problems, initialization is critical for their functional performance.

Based on our observation during measurement evaluations, CLEAN may evaluate many MPCs in the strongest cluster without detecting long-distance clusters even when the clusters are well-separated. This issue particularly occurs in the presence of calibration errors or diffuse scattering. Consequently, dozens of MPCs may be assigned to the strong clusters, while long-distance clusters may be missed completely; note that later iteration rounds of SAGE or RIMAX will not recover the clusters not initialized by CLEAN.

In this paper, we propose a new version of the CLEAN algorithm, regional CLEAN (R-CLEAN), to solve the problem heuristically. We compare R-CLEAN with traditional CLEAN for several synthetic channels and an actual THz outdoor measurement and show how the performance improves.

II. Signal model

The channel in the far-field of antennas can be expressed as the superposition of N_{path} planar waves (MPCs). The MIMO transfer function matrix of the channel [9] at a specific frequency point, f_k, can be expressed in terms of the MPC parameters as

$$\mathbf{H}(f_k) = \sum_{n=1}^{N_{\mathrm{path}}} \gamma_n \tilde{\mathbf{g}}_{\mathrm{R}}(\mathbf{\Omega}_{\mathrm{R},n}; f_k)\tilde{\mathbf{g}}_{\mathrm{T}}^T(\mathbf{\Omega}_{\mathrm{T},n}; f_k)e^{-j2\pi f_k \tau_n} + \mathbf{S}_{\mathrm{dmc}}(f_k) + \mathbf{N}(f_k), \tag{1}$$

where γ_n, $\mathbf{\Omega}_{\mathrm{R},n}$, $\mathbf{\Omega}_{\mathrm{T},n}$ and τ_n are complex amplitude, direction of arrival (DoA), direction of departure (DoD) and propagation delay, respectively, of the n-th MPC. The calibrated array patterns, $\tilde{\mathbf{g}}_{\mathrm{R}}(\mathbf{\Omega}_{\mathrm{R},n}; f_k) \in \mathbb{C}^{N_{\mathrm{R}}\times 1}$ and $\tilde{\mathbf{g}}_{\mathrm{T}}(\mathbf{\Omega}_{\mathrm{T},n}; f_k) \in \mathbb{C}^{N_{\mathrm{T}}\times 1}$, express the angular response from a certain direction, $\mathbf{\Omega}_{\mathrm{R},n}$ and $\mathbf{\Omega}_{\mathrm{T},n}$, at a particular frequency f_k. The additive noise, $\mathbf{N}(f_k) \in \mathbb{C}^{N_{\mathrm{R}}\times N_{\mathrm{T}}}$, is assumed to follow the zero-mean complex Gaussian distribution with identical variance and are independent among entries in the matrix and frequencies.

To simplify the diffuse multipath components (DMC) discussion, the vectorized aggregation of DMC matrices over frequencies, $\mathbf{s}_{\mathrm{dmc}} = \mathrm{vec}\{[\mathbf{S}(f_1), \cdots, \mathbf{S}(f_K)]^T\} \in \mathbb{C}^{KN_{\mathrm{R}}N_{\mathrm{T}}\times 1}$, is defined, where K denotes the number of discrete frequency points. The DMC is also assumed to be zero-mean complex circularly symmetric Gaussian distribution with covariance matrix $\mathbf{R}$, i.e., $\mathbf{s}_{\mathrm{dmc}} \sim \mathcal{CN}(\mathbf{0}, \mathbf{R})$, with the correlation being determined by the dispersion in the delay and angular domains [4]. The parametric model for the DMC is commonly assumed to be exponentially decaying in delay, and following a *von Mises distribution* in angle [10]. The covariance matrix, $\mathbf{R}$, is assumed to be decomposable [4], [10], [11] as the Kronecker-product of covariance matrix in frequency domain , $\mathbf{R}_f \in \mathbb{C}^{K\times K}$, and covariance matrices of antenna array elements, $\mathbf{R}_{\mathrm{R}} \in \mathbb{C}^{N_{\mathrm{R}}\times N_{\mathrm{R}}}$ and $\mathbf{R}_{\mathrm{T}} \in \mathbb{C}^{N_{\mathrm{T}}\times N_{\mathrm{T}}}$, in form of

$$\mathbf{R} = \mathbf{R}_{\mathrm{T}} \otimes \mathbf{R}_{\mathrm{R}} \otimes \mathbf{R}_f, \tag{2}$$

where the operation $\otimes$ denotes the Kronecker product.

CLEAN is essentially a serial interference cancellation approach: during each iteration, it uses a ML estimator to extract one MPC and subtracts its contribution from the (residual) channel observation. The 3D tensor for residual channel observation at i-th iteration, denoted by $\mathcal{H}^{(i)} \in \mathbb{C}^{K\times N_{\mathrm{R}}\times N_{\mathrm{T}}}$, is the aggregation of matrices, $\mathbf{H}^{(i)}(f_k)$, to align along another dimension formulating a 3D tensor matrix. In the i-th iteration, a single MPC is estimated, whose contribution to the channel matrix (i.e., a single element of the sum in (1)) is defined as $\hat{\mathcal{H}}^{(i)}$. The estimated parameters, $\left[\hat{\gamma}, \hat{\mathbf{\Omega}}_{\mathrm{R}}, \hat{\mathbf{\Omega}}_{\mathrm{T}}, \hat{\tau}\right]^T$, are chosen such that they minimize the difference between the residual channel observation and the MPC contribution, $\min \sum_k \sum_{n_{\mathrm{R}}} \sum_{n_{\mathrm{T}}} \|\mathcal{H}^{(i)}_{k,n_{\mathrm{R}},n_{\mathrm{T}}} - \hat{\mathcal{H}}^{(i)}_{k,n_{\mathrm{R}},n_{\mathrm{T}}}\|^2$, where the subscripts of tensor, k, n_{R}, and n_{T}, refer to indices in the corresponding dimensions. The residual channel observation is updated by $\mathcal{H}^{(i+1)} = \mathcal{H}^{(i)} - \hat{\mathcal{H}}^{(i)}$.

The estimation of the MPC parameters is a nonlinear problem, so a closed-form expression of the solution is not available. Therefore, a grid search is applied to explore all possible combinations of parameters to find the maximum/minimum of the objective function, thereby limiting the performance by the grid resolution; to simplify, multi-dimensional grid searches can be replaced by sequences of one-dimensional searches [8].

The minimization of the mean square error (MSE) in the CLEAN algorithm is based on the assumption of Gaussian noise. The contribution of the other MPCs in the channel is also assumed to be complex Gaussian. Therefore, evaluating iteratively multiple MPCs can be done until the residual power is under a predefined threshold or a maximum MPC number is reached. However, the DMC and its covariance matrix are not considered in the optimization. This covariance matrix mismatch can bias the MPC estimation, which can cause problems in detecting clusters that are weak and have a large distance (in any of the Fourier domains) from the main cluster(s).

III. Regional CLEAN algorithm

The standard CLEAN algorithm can suffer from a concentration of the extracted paths in the strongest cluster. The reasons for this can be several: (i) the discretization of the grid prevents an accurate estimation of the path parameters. The subtraction of the path at the inaccurate delay/angle, limited by the searching grid resolution, results in a residual error that is fitted by ghost paths in later iterations, which gives rise to more errors, and error propagation occurs. (ii) calibration errors of the channel impulse response lead to the subtraction of the ”wrong” contribution of an MPC in an iteration step, again giving rise to ghost paths. (iii) the presence of DMC, which is often strongest around the strongest cluster, leads to many MPCs being used to emulate the DMC behavior; see also the discussion above. Since any CLEAN use has an upper limit on the total number of estimated MPCs, it can easily happen that most - or all - of those paths are allocated to the first cluster.

We, therefore, propose R-CLEAN which is a heuristic CLEAN-based algorithm. The pseudo-code of the proposed algorithm is shown in Alg. 1. R-CLEAN can be decomposed into two-layer: the outer layer detects and iterates among clusters; the inner layer is the CLEAN algorithm to evaluate MPCs. The capability of cluster detection guarantees that all clusters within a given power range are evaluated. The traditional CLEAN algorithm is deployed in the inner layer to provide a feasible and relatively low-complexity solution for the initialization. R-CLEAN detects the position of clusters

1 **Input:** channel observation $\mathcal{H}$
2 **Output:** estimated MPC parameters
3 initialization: $\mathcal{H}_0 = \mathcal{H}$, $i = 0$, $ADPS$ from $\mathcal{H}_0$;
4 **while** *detect a cluster from* $ADPS$ **do**
5   localize $ADPS$ maximum;
6   generate search grid around cluster center ;
7   **while** *not MPCs number or residue power* **do**
8   estimate MPC parameters using CLEAN
      end
9   aggregate estimated MPC parameters;
10     $i \leftarrow i + 1$;
11   update channel residue $\mathcal{H}_i$;
12   compute $ADPS$ from $\mathcal{H}_i$;
end

Algorithm 1: Pseudo-code of R-CLEAN algorithm

based on the Fourier analysis of the channel observations. The maximum of the angular delay power spectrum (ADPS) is used to detect the cluster and initialize the cluster position. A multi-dimensional searching grid is initialized around this area after detecting such a maximum, which can be called the cluster center. If the cluster center is well-separated from the others, at least 2 Fourier resolutions - the inverse of bandwidth in delay and half-power beamwidth in angle - away in any parameter domains, a new cluster is detected (Alg. 1, line 4). The size of the search area (*cluster size*) can be determined by the number of Fourier resolutions at the cluster center.

As mentioned above, the traditional CLEAN algorithm is deployed to evaluate the MPC parameters for each detected cluster. Our implementation of the CLEAN algorithm is alternating between parameter domains to reduce complexity [8]. Provided the search grids are limited to a local region, the local minimizer is guaranteed to concentrate on a specific cluster.

Corresponding to line 7 in Alg. 1, the CLEAN evaluation will be halted if one of the following conditions is satisfied: i) the ADPS level of the detected cluster is lower than a preselected threshold; ii) the number of extracted MPCs reaches a predefined value. If the ADPS after the extraction of all the evaluated MPCs at the detected position is lower than a threshold, e.g., 30 dB, it could be regarded as a "clean" extraction of the cluster. On the other hand, if the number of MPCs evaluated at a cluster reaches the maximum MPC number, estimation of further paths can still improve the MSE but might "use up" the (limited by design) number of total available MPCs for the channel estimation.

The detection and evaluation for clusters in the channel observation continue until the detected maximum in ADPS is lower than a power threshold. The number of "visible" clusters depends on the dynamic range related to the noise level and/or dynamic range. If the dynamic range is relatively low, e.g., 10 dB below the ADPS maximum, then the LOS or the strongest cluster might be the only cluster that is detected. In contrast, a larger dynamic range will lead to the detection of more clusters. Given the same number of extracted MPCs, the computational complexity of R-CLEAN is comparable to conventional CLEAN algorithm.

IV. Numerical results

This section presents the performance comparison between CLEAN and R-CLEAN on three synthetic channels and one LOS THz outdoor measurement.

A. Evaluated parameters

First and foremost, we present the power delay profile (PDP) results and which clusters are detected by the different algorithms. While similar effects can also be observed in the angular domain, space constraints prevent the graphic representation of those results.

Missing long-delayed clusters has a powerful impact on the *RMS delay spread*, i.e., the second central moment of the PDP, a widely accepted measure of delay dispersion [2]. Since the actual value of the RMS delay spread is not directly available from measurements, it cannot be compared to the value obtained from CLEAN. The *measured* PDP can be regarded as the impulse response of the sounding system convolved with the channel. The measured RMS delay spread is thus the second central moment of the measured PDP.

Given that the measured RMS delay spread can be impacted by noise, we apply noise thresholding, i.e., set the average PDP (APDP) to zero when weaker than a pre-selected threshold. Therefore, the clusters above the threshold contribute to the statistics. Furthermore, contributions with delays larger than a particular threshold are not considered, which is also known as delay gating. The main motivation for delay gating is to avoid sidelobes of strong early MPCs (e.g., a LOS component) that, due to the periodicity of a fast Fourier transform (FFT), can *wrap around* and appear at long delays.

We furthermore define the *filtered* PDP as the convolution of the channel as estimated from CLEAN (i.e., sequence of delta pulses) with the impulse response of the sounding signal, and the *filtered RMS delay spread*, denoted by $\tilde{S}_{\tau}$, as the second central moment of this filtered PDP. The filtered RMS delay spread is better for the delay dispersion than the delay spread computed from the delta pulses (directly taken from CLEAN) MPCs. CLEAN might extract MPCs that are similar in magnitude but almost out of phase to best fit a measurement result. However, in the PDP, only power is considered so that the "power combination" of two delta pulses can deviate significantly from the power obtained by phase-correct filtering of the MPCs. In contrast, the filtered RMS delay spread measures the filtered (i.e., reconstructed) PDP. The phase of delta pulses is hidden in the filtered PDP (as it is in the measured PDP), so the problem is overcome. Furthermore, it also provides a feasible metric for cluster detection, both the channel observation and the estimation.

B. Synthetic channels

We generate synthetic channels that have three clusters with different MPC parameters. The average delays for those three clusters are 6 m, 30 m, and 100 m. The average DoD and DoA for each cluster are 10°, 70°, and 40°, respectively. For both the channel generation and the extraction in the simulation, we use the measured (in an anechoic chamber) pattern of a horn antenna whose half-power beamwidth is approximately 10°. The synthetic channel is "measured" by a virtual array with 36 antennas at both ends with uniform spacing of 10°. The average random MPC magnitude for each cluster is set to be -5 dB, -20 dB, and -45 dB. There are 2 MPCs in the first and second cluster and 3 MPCs in the third cluster.

These same synthetic channels are used with different possible model mismatches - calibration error in the impulse response, antenna pattern calibration error, and DMC in the channel. With those synthetic channels, performance comparisons of CLEAN and R-CLEAN algorithms are deployed. The baseline in Table I refers to the RMS delay spread of the measured PDP of the channel.

C. Calibration error in frequency response

A calibration error may exist in the impulse response due to noise, reflections at cable interfaces, temperature drift, and other component variations during calibration. It can result in pre-cursors and post-cursors that affect the shape of the system impulse response. This effect is equivalent to convolving a different filter function $g(f)$ for the generation of the channel and the analysis. Therefore, the calibration error in the impulse response is emulated, as shown in Fig. 1a. The blue line shows the simulated calibration error with a pre-cursor and post-cursors. The continuous part of the impulse response level is also different from the pulse without calibration error as the red line in the figure.

The evaluation comparison of CLEAN and R-CLEAN is shown in Fig. 2a. We make the evaluation results comparable by extracting 30 MPCs with any of the algorithms. R-CLEAN will evaluate six peaks in the APDP with 5 MPCs in each detected peak. With a fixed number of MPCs, CLEAN does

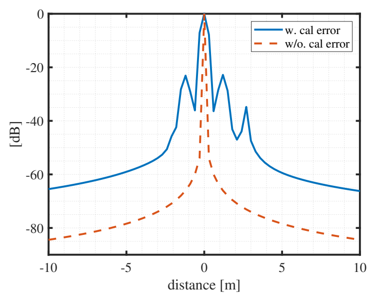

(a) Simulated calibration error in impulse response.

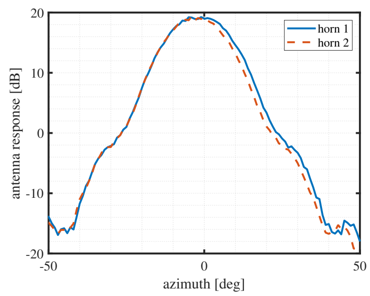

(b) Different antenna patterns to emulate pattern calibration error.

Fig. 1: Two types of calibration error.

TABLE I: Filtered RMS delay spread (in meters) comparison for channels.

Method	synthetic channel 1	synthetic channel 2	synthetic channel 3	THz outdoor
baseline	3.53	2.60	4.41	8.22
CLEAN	1.15	0.54	0.70	7.40
R-CLEAN	2.90	2.46	3.34	7.64

not evaluate the second and third clusters. However, R-CLEAN can detect all those three clusters, even though the third cluster falls into the noise. The first column of Table I shows that R-CLEAN decreases the difference between filtered and the measured RMS delay spread. The pre-cursors and post-cursors in the calibration error have changed the shape of APDP as shown in Fig. 2a.

D. Imperfect antenna pattern calibration

Like the impulse response calibration, the effective antenna pattern during measurements might differ from the calibrated pattern. This variation can occur, e.g., due to mechanical distortion (expansion in heat), material corrosion, misalignment compared to the assumed direction, and errors during the actual calibration process. In our simulations, we use two different patterns for the generation of the synthetic channel impulse response and the parameter extraction, Fig. 1b shows that the patterns are similar except for a constant difference from 0° to 45°.

The comparison of the evaluation results from CLEAN and R-CLEAN is shown in Fig. 2b. Again, 30 MPCs are selected to be evaluated with different algorithms. R-CLEAN will evaluate six peaks in the APDP with 5 MPCs in each detected peak. Due to the effects described in Sec. III, CLEAN does not evaluate the second and third clusters. On the other hand, R-CLEAN can detect all three clusters. In Table I, it is shown that R-CLEAN decreases the filtered RMS delay spread difference to a large degree. The reconstructed channel estimated by R-CLEAN provides a closer value of filtered RMS delay spread to the measured spread.

E. Channel with DMC existence

The DMC is a single-exponential decay, starting at the first cluster, i.e., at 6 m. For simplicity, the distribution of the DMC in the angular domain is assumed to be uniform. In Fig. 2c, the average PDP between 6 and 50 meters corresponds to the DMC with exponential decay (linear decay on a dB scale). The peak of the DMC has comparable power compared to the second cluster. Therefore, it creates difficulties in evaluating the weak clusters.

The comparison of the evaluation results from CLEAN and R-CLEAN is shown in Fig. 2c. Similar to our previous evaluations, we evaluated 30 MPCs with different algorithms, with R-CLEAN evaluating up to 6 peaks in the APDP with 5 MPCs in each detected peak. With a fixed number of MPCs, only the first cluster is detected and evaluated by CLEAN. The second cluster is detected with R-CLEAN, while an amount of power is left in the residue as the initialization for DMC. The third column of Table I shows that R-CLEAN improves the agreement of RMS delay spread significantly. CLEAN only concentrates on the first cluster and DMC with significant power so that the filtered RMS delay spread is as small as 0.7 m. Furthermore, the measured (and the R-CLEAN-extracted, filtered) RMS delay spread is larger than the values in the other synthetic channels since the DMC with significant power contributes to the second-order characteristics.

F. THz outdoor measurement

The THz (145 - 146 GHz) channel we analyze is taken from an outdoor measurement campaign conducted on the campus of the University of Southern California [12]. A line-of-sight (LOS) scenario with a distance of 37 m between Tx and Rx is selected for evaluation. Two horn antennas are placed on rotors to measure the channel with 10° steps at the Tx and Rx. The aggregation of the channel observations is equivalent to a 36-by-36 MIMO array; the measured bandwidth is 1 GHz, sweeping over 1001 frequency points. The investigated delay range is limited to 150 m distance since MPCs with larger run-length fall under the noise threshold.

The comparison of CLEAN and R-CLEAN is shown in Fig. 3. A maximum of 130 MPCs are selected to be evaluated with the different algorithms. R-CLEAN will evaluate 13 peaks in the APDP with 10 MPCs for each detected peak in ADPS. CLEAN only detects and evaluates 4 clusters, while R-CLEAN distinguishes 8 clusters with significant power. It is evident from Fig. 3 that more clusters with considerable power are detected with R-CLEAN. The last column of Table I shows that R-CLEAN improves the agreement between reconstructed and measured filtered RMS delay spread. The four clusters detected by CLEAN cover approximately 20 dB dynamic range,

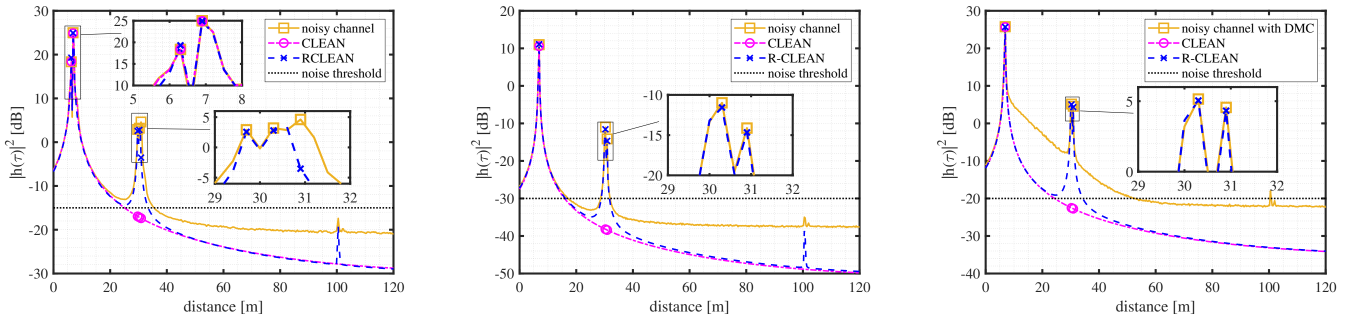

(a) Evaluation of synthetic channel with calibration error in impulse response. Noise threshold is -15 dB.

(b) Evaluation of synthetic channel with pattern calibration error. Noise threshold is -30 dB.

(c) Evaluation of synthetic channel with DMC. Noise threshold is -20 dB.

Fig. 2: APDP comparison between channel, estimation from CLEAN and R-CLEAN.

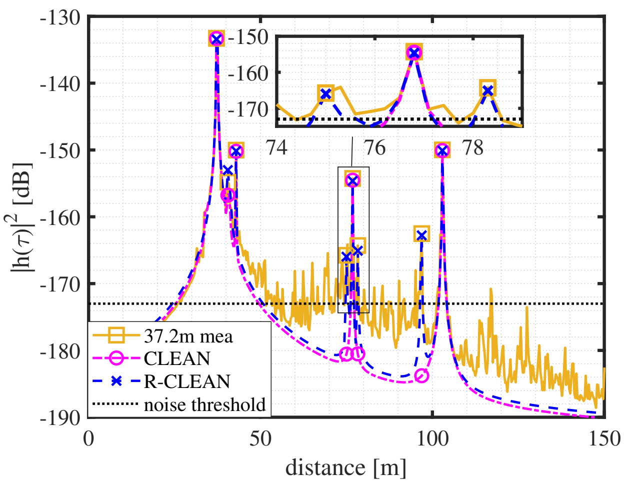

Fig. 3: Evaluation of outdoor LOS measurement at 37m. The noise threshold selection guarantees a 40 dB dynamic range.

which prevents us from exploring channel models with larger dynamic ranges to best describe the channel. The evaluation by CLEAN also demonstrates the observed problem, namely the concentration within stronger clusters, which is the inspiration of the proposed algorithm.

V. Conclusion

This paper proposes a new channel estimation algorithm to detect even weak, long-delayed clusters of MPCs when applying high-resolution parameter estimation. A CLEAN-based algorithm, named regional CLEAN, provides a heuristic solution to the dilemma that regular CLEAN can get "stuck" in the strongest cluster, estimating more and more ghost paths there while ignoring later, weaker clusters. R-CLEAN is validated on three synthetic channels with different calibration errors and DMC types. Evaluation of a sample THz channel measurement in an outdoor environment also demonstrates its capability for cluster detection. R-CLEAN leads to filtered RMS delay spread values that show better agreement with the measured values. R-CLEAN also provides the capability to initialize components for further improvement by RIMAX.

Acknowledgment

The work of USC was supported by the Semiconductor Research Corporation (SRC) under the ComSenTer program, the National Institute of Standards and Technology, the National Science Foundation, Samsung Research America, and the Foreign Fulbright Ecuador SENESCYT Program.

References

[1] H. Tataria, M. Shafi, A. F. Molisch, M. Dohler, H. Sjöland, and F. Tufvesson, "6g wireless systems: Vision, requirements, challenges, insights, and opportunities," *Proceedings of the IEEE*, vol. 109, pp. 1166–1199, 2021.

[2] A. F. Molisch, *Wireless communications*. IEEE Press - John Wiley & Sons, 2nd ed., 2012.

[3] B. H. Fleury, M. Tschudin, R. Heddergott, D. Dahlhaus, and K. I. Pedersen, "Channel parameter estimation in mobile radio environments using the SAGE algorithm," *IEEE J. Sel. Areas Commun.*, vol. 17, pp. 434–450, 1999.

[4] A. Richter, *Estimation of radio channel parameters: Models and algorithms*. Ph.d. dissertation, Technische Universität Ilmenau, Ilmenau, Germany, 2005.

[5] R. S. Thoma, M. Landmann, G. Sommerkorn, and A. Richter, "Multidimensional high-resolution channel sounding in mobile radio," in *Proceedings of the 21st I2MTC*, pp. 257–262, 2004.

[6] J. Högbom, "Aperture synthesis with a non-regular distribution of interferometer baselines," *Astronomy and Astrophysics Supplement Series*, vol. 15, p. 417, 1974.

[7] R.-M. Cramer, R. A. Scholtz, and M. Z. Win, "Evaluation of an ultra-wide-band propagation channel," *IEEE Trans. Antennas Propag.*, vol. 50, pp. 561–570, 2002.

[8] V. Kristem, S. Sangodoyin, C. U. Bas, M. Käske, J. Lee, C. Schneider, G. Sommerkorn, C. J. Zhang, R. S. Thomä, and A. F. Molisch, "3D MIMO outdoor-to-indoor propagation channel measurement," *IEEE Trans. Wireless Commun.*, vol. 16, pp. 4600–4613, 2017.

[9] M. Steinbauer, A. F. Molisch, and E. Bonek, "The double-directional radio channel," *IEEE Antennas Propag. Magazine*, vol. 43, pp. 51–63, 2001.

[10] S. Sangodoyin, V. Kristem, C. U. Bas, M. Käske, J. Lee, C. Schneider, G. Sommerkorn, C. J. Zhang, R. Thomä, and A. F. Molisch, "Cluster characterization of 3-D MIMO propagation channel in an urban macrocellular environment," *IEEE Trans. Wireless Commun.*, vol. 17, pp. 5076–5091, 2018.

[11] S. Sangodoyin, M. Kerpicci, C.-L. Cheng, and A. Zajić, "High-resolution spatio-temporal evaluation of specular and diffuse paths in thz mimo channels," in *2021 URSI GASS*, pp. 1–4, IEEE.

[12] N. A. Abbasi, J. Gomez-Ponce, R. Kondaveti, S. M. Shaikbepari, S. Rao, S. Abu-Surra, G. Xu, C. Zhang, and A. F. Molisch, "Thz band channel measurements and statistical modeling for urban d2d environments," *arXiv preprint arXiv:2109.13693*, 2021.